NAV AIR

Weibull Analysis and Area Scaling for Infrared Window Materials

by
Daniel C. Harris
Research Division
Research and Engineering Group

AUGUST 2016

**NAVAL AIR WARFARE CENTER WEAPONS DIVISION
CHINA LAKE, CA 93555-6100**

Naval Air Warfare Center Weapons Division

FOREWORD

This report provides a tutorial on the Weibull distribution of strength of ceramic materials and the use of the maximum likelihood method of American Society for Testing and Materials (ASTM) C1239 to obtain Weibull parameters from a set of test coupons. Parameters compiled from test data of infrared window materials are used to predict the static probability of failure of an optical window in the absence of slow crack growth. This report emphasizes how the strength of a window scales inversely with the size of the window.

This report was reviewed for technical accuracy by Howard Poisl, Thomas M. Hartnett, and Lee M. Goldman.

Approved by
A. VAN NEVEL, *Head*
Research Division
4 August 2016

Under authority of
B. K. COREY
RDML, U.S. Navy
Commander

Released for publication by
J. L. JOHNSON
Director for Research and Engineering

1. REPORT DATE *(DD-MM-YYYY)*	2. REPORT TYPE	3. DATES COVERED (From - To)
04-08-2016	Final	1 October 2015–6 July 2016

4. TITLE AND SUBTITLE	5a. CONTRACT NUMBER
Weibull Analysis and Area Scaling for Infrared Window Materials (U)	N/A
	5b. GRANT NUMBER N/A
	5c. PROGRAM ELEMENT NUMBER N/A

6. AUTHOR(S)	5d. PROJECT NUMBER
Daniel C. Harris	N/A
	5e. TASK NUMBER N/A
	5f. WORK UNIT NUMBER N/A

7. PERFORMING ORGANIZATION NAME(S) AND ADDRESS(ES)	8. PERFORMING ORGANIZATION REPORT NUMBER
Naval Air Warfare Center Weapons Division 1 Administration Circle China Lake, California 93555-6100	NAWCWD TP 8806

9. SPONSORING/MONITORING AGENCY NAME(S) AND ADDRESS(ES)	10. SPONSOR/MONITOR'S ACRONYM(S)
Office of Naval Research 875 North Randolph Street Arlington, Virginia 22203	ONR
	11. SPONSOR/MONITOR'S REPORT NUMBER(S) N/A

12. DISTRIBUTION/AVAILABILITY STATEMENT

DISTRIBUTION STATEMENT A. Approved for public release.

13. SUPPLEMENTARY NOTES
None.

14. ABSTRACT

(U) This report provides a tutorial on the Weibull distribution of strength of ceramic materials and the use of the maximum likelihood method of American Society for Testing and Materials (ASTM) C1239 to obtain Weibull parameters from a set of test coupons. Parameters compiled from test data of infrared window materials are used to predict the static probability of failure of an optical window in the absence of slow crack growth. This report emphasizes how the strength of a window scales inversely with the size of the window. Test data are given for aluminum oxynitride (ALON), calcium fluoride, chemical vapor deposited (CVD) diamond, fused quartz, germanium, magnesium fluoride, yttria-magnesia nanocomposite optical ceramic (NCOC), polycrystalline alumina, sapphire (*a*-plane, *c*-plane, and *r*-plane), magnesium aluminum spinel, yttria, zinc selenide, and zinc sulfide (standard and multispectral grades).

15. SUBJECT TERMS
ALON, Aluminum Oxynitride, Area Scaling of Strength, ASTM C1239, Calcium Fluoride, Ceramic Mechanical Strength, CVD Diamond, Fused Quartz, Germanium, Magnesium Fluoride, Maximum Likelihood Method, NCOC, Polycrystalline Alumina, Sapphire, Spinel, Static Probability of Failure, Weibull Analysis, Yttria, Yttria-Magnesia Nanocomposite Optical Ceramic, Zinc Selenide, Zinc Sulfide

16. SECURITY CLASSIFICATION OF:			17. LIMITATION OF ABSTRACT	18. NUMBER OF PAGES	19a. NAME OF RESPONSIBLE PERSON Daniel C. Harris
a. REPORT UNCLASSIFIED	**b. ABSTRACT** UNCLASSIFIED	**c. THIS PAGE** UNCLASSIFIED	SAR	36	**19b. TELEPHONE NUMBER** *(include area code)* (760) 939-1649

CONTENTS

EXECUTIVE SUMMARY

A tutorial is provided on the Weibull distribution of strength of ceramic materials and use of the maximum likelihood method of American Society for Testing and Materials (ASTM) C1239 to obtain Weibull parameters from test data. Parameters are compiled from testing of the infrared window materials aluminum oxynitride (ALON), calcium fluoride, chemical vapor deposited (CVD) diamond, fused quartz, germanium, magnesium fluoride, yttria-magnesia nanocomposite optical ceramic (NCOC), polycrystalline alumina, sapphire (*a*-plane, *c*-plane, and *r*-plane), magnesium aluminum spinel, yttria, zinc selenide, and zinc sulfide (standard and multispectral grades). Weibull parameters are used to predict the static probability of failure of an optical window in the absence of slow crack growth. This report illustrates how the strength of a window scales inversely with the size of the window.

This page intentionally left blank.

INTRODUCTION

The most common description of failure statistics for infrared window materials is the Weibull distribution (References 1 and 2). By measuring the strengths of a sufficiently large set of specimens, we seek to answer the question "What is the probability that a sufficiently large flaw is present to initiate failure at a particular applied stress in a particular size of window?" Our discussion assumes that there is a single population of surface flaws from which failure originates.

WEIBULL EQUATION IN AMERICAN SOCIETY FOR TESTING AND MATERIALS (ASTM) C1239

When a set of coupons is broken in a flexure test of mechanical strength, we observe a range of strengths. The cumulative probability of failure (P_f) describing the observed set of strengths usually follows the Weibull distribution shown in Figure 1:

Weibull equation with characteristic strength σ_θ
$$P_f = 1 - e^{-\left(\frac{\sigma}{\sigma_\theta}\right)^m}$$
(1)

where σ is the applied tensile stress, σ_θ is called the *Weibull characteristic strength*, and m is the *Weibull modulus*. The strength of each coupon is taken as the maximum stress in the central region of the tensile face at the time of failure.
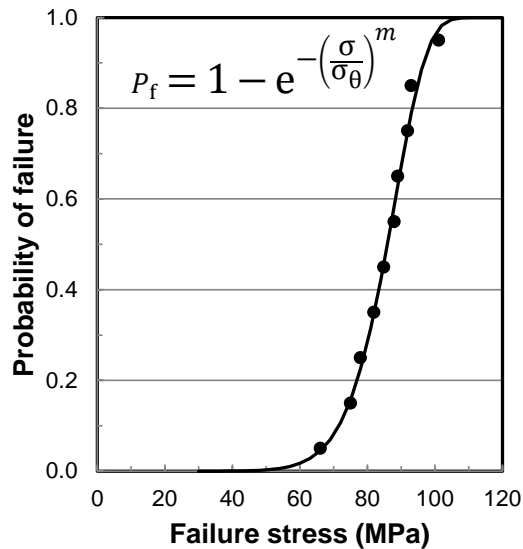
FIGURE 1. Weibull Curve (Cumulative Probability of Failure) Fit to Observed Strengths (Failure Stress) of 10 Test Coupons.

The cumulative probability of failure P_f ranges from 0 at low stress to 1 at sufficiently high stress in Figure 1. The spread of strengths is related to the Weibull modulus, *m*, which is typically in the range 3 to 15 for polished optical ceramics. The larger the value of *m*, the narrower is the distribution of strength. A narrow distribution of strengths (a large Weibull modulus) is desirable for a reliable mechanical design. The greater the characteristic strength, σ_θ, the greater is the mean strength of the set of coupons.

Weibull characteristic strength σ_θ in Equation 1 is not a material property. It depends on specimen size, the type of mechanical test, and the dimensions of the test fixture. If specimens fail from surface flaws, the *effective area* under tension (A_e) can be incorporated into the Weibull equation. *In a given mechanical test at a particular stress, a specimen of effective area A_e has the same probability of failure as a sample with geometric area A_e loaded in uniform uniaxial tension*. Effective area accounts for the kind of test being done and for specimen size and test fixture dimensions:

Weibull equation with Weibull scale factor σ_o
$$P_f = 1 - e^{-\left(\frac{A_e}{A_0}\right)\left(\frac{\sigma}{\sigma_o}\right)^m} \tag{2}$$

Equation 2 incorporates effective area A_e and contains the *Weibull scale factor* σ_o in place of the characteristic strength σ_θ. The scale factor σ_o is ideally a property of the material and the way it is fabricated. In the exponent of Equation 2, A_o is taken as one unit of area, such as 1 cm^2, to cancel the units of A_e, because an exponent must be dimensionless. Equating exponents in Equations 1 and 2 provides the relationship between the material property σ_o and the curve-fitting parameter σ_θ from Figure 1:

$$\underbrace{-\left(\frac{\sigma}{\sigma_\theta}\right)^m}_{\text{Eq. (1)}} = \underbrace{-\left(\frac{A_e}{A_0}\right)\left(\frac{\sigma}{\sigma_o}\right)^m}_{\text{Eq. (2)}} \Rightarrow \sigma_o = \sigma_\theta \left(\frac{A_e}{A_0}\right)^{1/m} \tag{3}$$

The symbol "$\Rightarrow$" is read "implies that". The Weibull scale factor σ_o is the Weibull characteristic strength when the effective area of the specimen is 1 cm^2.

The expected mean strength of replicate samples with effective area A_e is

$$\text{Expected mean strength} = \sigma_o \left(\frac{A_0}{A_e}\right)^{1/m} \Gamma\left(1 + \frac{1}{m}\right) \tag{4}$$

where Γ is the gamma function of the argument $(1 + 1/m)$. You can compute the numerical value of Γ in an Excel® spreadsheet with the statement "=exp(gammaln(1+1/m))".[*]

σ_θ: **Weibull characteristic strength** obtained by fitting strengths of test specimens to Equation 1.

σ_o: **Weibull scale factor** computed from σ_θ with Equation 3. σ_o would be the characteristic strength if test samples had an effective area of $A_e = 1$ cm^2.

Caveat Emptor. There is inconsistent use of the symbols σ_θ and σ_o and the terms "characteristic strength" and "scale factor" in the literature. *It is impeccable practice to write the Weibull equation that you are using and to write the names of the different symbols.*

EFFECTIVE AREA A_e

RING-ON-RING GEOMETRY

Consider the ring-on-ring equibiaxial flexure test of a ceramic disk with radius c in Figure 2. The disk is pressed from above by the small load ring of radius a and supported from below by the large support ring of radius b. There is tensile stress on the support surface and compressive stress on the load surface. Failure initiates on the tensile surface. On each surface, there are radial and hoop components of stress.

Load radius = a = 0.80 cm
Support radius = b = 1.60 cm
Disk radius = c = 1.90 cm
Disk thickness = h = 0.20 cm
Poisson's ratio = ν = 0.30

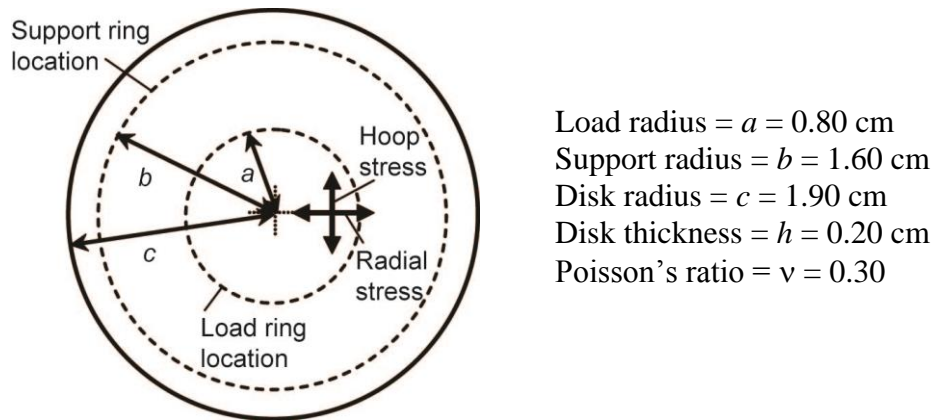FIGURE 2. Geometry of Ring-on-Ring Flexure Test of a Polished Ceramic Disk.

---

[*]The gamma function is $\Gamma\left(1 + \frac{1}{m}\right) = \int_0^\infty t^{1/m}\, e^{-t}dt$, which is near unity. For $m = 5$, $\Gamma\left(1 + \frac{1}{5}\right) = 0.918$. For $m = 10$, $\Gamma = 0.951$ and for $m = 15$, $\Gamma = 0.966$. For integer arguments n, gamma is the factorial function $\Gamma(n) = (n-1)!$.

The effective area in tension A_e is required for Weibull Equation 2. With the approximation that each component of tensile stress acts independently to open a crack, the effective area is defined by the integral

*Effective area for
 biaxial tension*
$$A_\mathrm{e} = \int_A \left[\left(\frac{\sigma_\mathrm{hoop}}{\sigma_{max}} \right)^m + \left(\frac{\sigma_\mathrm{radial}}{\sigma_{max}} \right)^m \right] dA \tag{5}$$

where m is the Weibull modulus and A is area. The two components of stress are σ_hoop and σ_radial. The maximum stress in the central region of the tensile surface is σ_max. Integration is carried out on the tensile surface inside support radius b in Figure 2. For the ring-on-ring flexure test, integration of Equation 5 gives the effective area (Reference 3)

*Effective area for
ring-on-ring test*
$$A_\mathrm{e} = 2\pi a^2 \left\{ \frac{44(1+\nu)}{3(1+m)} \frac{5+m}{2+m} \left(\frac{b-a}{bc} \right)^2 \left[\frac{2c^2(1+\nu)+(b-a)^2(1\text{-}\nu)}{(3+\nu)(1+3\nu)} \right] \right\} \tag{6}$$

where m is the Weibull modulus and ν is Poisson's ratio.

Example: Effective and geometric areas of flexure disks. Compare the geometric area in tension to the effective area in tension for the ring-on-ring flexure test in Figure 2 with Poisson's ratio $\nu = 0.30$, and Weibull modulus $m = 5$ or 10.

The *geometric area* in tension is the area inside the support ring $= \pi b^2 = \pi(1.6 \text{ cm})^2 = 8.04 \text{ cm}^2$. The area inside the load ring, called the *inner gauge area*, is $\pi(0.8 \text{ cm})^2 = 2.01 \text{ cm}^2$. The *effective area in tension*, given by Equation 6, is:

$$A_\mathrm{e} = 2\pi a^2 \left\{ 1 + \frac{44(1+\nu)}{3(1+m)} \frac{5+m}{2+m} \left(\frac{b-a}{bc} \right)^2 \left[\frac{2c^2(1+\nu)+(b-a)^2(1\text{-}\nu)}{(3+\nu)(1+3\nu)} \right] \right\}$$

$$A_\mathrm{e} = 2\pi(0.8)^2 \left\{ 1 + \frac{44(1+0.30)}{3(1+5)} \frac{5+5}{2+5} \left(\frac{1.6-0.8}{(1.6)(1.9)} \right)^2 \left[\frac{2*1.9^2(1+0.30)+(1.6-0.8)^2(1\text{-}0.30)}{(3+0.30)(1+3*0.30)} \right] \right\} = 6.00 \text{ cm}^2.$$

For a Weibull modulus $m = 10$, the effective area is reduced to 4.97 cm². The effective area is in between the geometric area of the load ring and the geometric area of the support ring.

PRESSURE-ON-RING GEOMETRY

Now consider the circular sensor window in Figure 3 with a uniform pressure applied to the left side. The right side will be in tension. Let the window radius be c and the radius of the retaining gasket be b. The effective area is (Reference 4)

Effective area for pressure-on-ring geometry

$$A_e \approx \frac{4\pi(1+\nu)}{1+m} \left(\frac{b}{c}\right)^2 \left[\frac{2c^2(1+\nu)+b^2(1-\nu)}{(3+\nu)(1+3\nu)}\right]$$ (7)
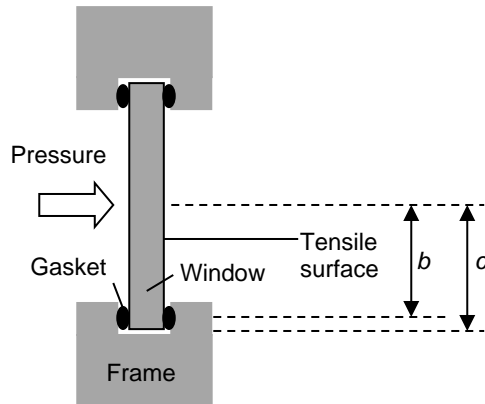
FIGURE 3. Side View of Circular Sensor Window Subjected
to a Uniform Pressure Difference Between the Two Faces.
This geometry is called *pressure on ring*.

With the same support and disk diameter as the ring-on-ring test in Figure 2 ($b = 1.60$ cm and $c = 1.90$ cm), the effective area for pressure-on-ring flexure for Weibull modulus $m = 5$ is given by Equation 7:

$$A_e \approx \frac{4\pi(1+0.30)}{1+5} \left(\frac{1.6}{1.9}\right)^2 \left[\frac{2*1.9^2(1+0.30)+1.6^2(1-0.30)}{(3+0.30)(1+3*0.30)}\right] = 3.44 \text{ cm}^2.$$

For $m = 10$, A_e is reduced to 1.88 mm^2.

The effective area for pressure-on-ring geometry is about half of the effective area for ring-on-ring geometry because stresses (σ_{hoop} and σ_{radial} in Equation 5) in pressure-on-ring geometry fall off more rapidly than they do in ring-on-ring geometry. In both geometries, A_e is less than the geometric area within the support ring and A_e decreases as the Weibull modulus increases.

WEIBULL ANALYSIS IN ASTM C1239

Now we seek to find the parameters m and σ_θ in Weibull Equation 1 to fit the strengths of 10 ceramic disks in Figure 1. ASTM C1239 prescribes that the *maximum likelihood method* should be used for this purpose. Work is set out in Figure 4. Equibiaxial flexure strengths (observed stress at failure) are listed *in order of increasing stress* in cells B5:B14. Column A assigns a number $i = 1$ to 10 to each specimen. The total number of samples is $n = 10$ in cell B16. Cells C5:C14 give the probability of failure for each specimen, defined as

$$\text{Probability of failure } (P_\text{f}) \equiv \frac{i-0.5}{n} \tag{8}$$

Equation 8 divides the range 0 to 1 into $n = 10$ equal intervals.

	A	B	C	D	E	F
1		x	y			
2		Failure	Probability	Components of maximum likelihood		
3	Sample	stress	of failure	fit to Weibull equation		
4	number (i)	σ (MPa)	P_f = (i-0.5)/n	σ^m	$\ln(\sigma)$	$\sigma^m \ln(\sigma)$
5	1	66.1	0.0500	8.321E+10	4.191	3.487E+11
6	2	75.0	0.1500	1.779E+11	4.317	7.682E+11
7	3	77.9	0.2500	2.237E+11	4.356	9.744E+11
8	4	81.9	0.3500	3.024E+11	4.406	1.332E+12
9	5	84.8	0.4500	3.731E+11	4.441	1.657E+12
10	6	87.9	0.5500	4.612E+11	4.476	2.065E+12
11	7	89.0	0.6500	4.969E+11	4.489	2.230E+12
12	8	91.9	0.7500	6.016E+11	4.520	2.720E+12
13	9	92.9	0.8500	6.447E+11	4.532	2.922E+12
14	10	101.1	0.9500	1.069E+12	4.616	4.933E+12
15			sum =	4.433E+12	44.344	1.995E+13
16	n =	10				
17	m =	6	←Guess m in cell B17 and solve for maximum			
18			likelihood value of m to make sum in cell D22 = 0			
19						
20	$\dfrac{\sum_{i=1}^{n} \sigma_i^m \ln(\sigma_i)}{\sum_{i=1}^{n} \sigma_i^m} - \dfrac{1}{n}\sum_{i=1}^{n}\ln(\sigma_i) - \dfrac{1}{m} = 0$				(A)	
21						
22		Sum of terms in Eq. (A) =		-0.101191847		
23						
24	$\sigma_\theta = \left[\dfrac{1}{n}\sum_{i=1}^{n}(\sigma_i^m)\right]^{1/m} =$			87.3		(B)
25						

FIGURE 4. Initial Excel Spreadsheet With a Guess $m = 6$
for the Weibull Modulus in Cell B17.

The maximum likelihood method outlined near the end of this report provides a pair of equations that we solve for m and σ_θ in the spreadsheet:

Maximum likelihood equations:

$$\frac{\sum_{i=1}^{n} \sigma_i^m \ln(\sigma_i)}{\sum_{i=1}^{n} \sigma_i^m} - \frac{1}{n}\sum_{i=1}^{n} \ln(\sigma_i) - \frac{1}{m} = 0 \tag{9}$$

$$\sigma_\theta = \left[\frac{1}{n}\sum_{i=1}^{n}(\sigma_i^m)\right]^{1/m} \tag{10}$$

The spreadsheet in Figure 4 begins with a *guess* of the value $m = 6$ for the Weibull modulus in cell B17. The guess does not have to be good for the spreadsheet to work. With the guess $m = 6$, Excel computes the quantities σ^m, $\ln \sigma$, and $\sigma^m \ln \sigma$ in columns D through F and sums in row 15. If we had guessed the correct value of m, the sum in Equation 9 would be 0. Instead, inserting sums from row 15 into Equation 9 gives

$$\frac{\sum_{i=1}^{n} \sigma_i^m \ln(\sigma_i)}{\sum_{i=1}^{n} \sigma_i^m} - \frac{1}{n}\sum_{i=1}^{n} \ln(\sigma_i) - \frac{1}{m} =$$

$$\frac{1.995 \times 10^{13}}{4.433 \times 10^{12}} - \frac{1}{10}(44.344) - \frac{1}{6} = -0.10119 \tag{9}$$

The guess $m = 6$ gives a sum of –0.10119 for Equation 9 in cell D22.

You can use either of two Excel procedures, Solver or Goal Seek, to vary m in cell B17 until the sum in cell D22 is 0, giving $m = 10.280$, which, in turn, gives the characteristic strength $\sigma_\theta = 89.0$ MPa from Equation 10 in cell D24 of Figure 5.

The value $\sigma_\theta = 89.0$ MPa is considered to be a good estimate. However, there is statistical bias in the value of m for small data sets (References 5 and 6). ASTM C1239 instructs us to multiply the value of m from the maximum likelihood method by the *unbiasing factor* in Table 1 for the best estimate of the Weibull modulus:

$$m_{\text{unbiased}} = m \times unbiasing\ factor \tag{11}$$

For $n = 10$ test specimens in Table 1, the unbiasing factor is 0.859, so the unbiased estimate of m is

$$m_{\text{unbiased}} = 10.280 \times 0.859 = 8.83 \tag{12}$$

The unbiasing factor approaches 1 as the number of specimens becomes large. According to ASTM C1239, the "best" value of m is 8.83.

	A	B	C	D	E	F
1		x	y			
2		Failure	Probability	Components of maximum likelihood		
3	Sample	stress	of failure	fit to Weibull equation		
4	number (i)	σ (MPa)	$P_f = (i-0.5)/n$	σ^m	$\ln(\sigma)$	$\sigma^m\ln(\sigma)$
5	1	66.1	0.0500	5.128E+18	4.191	2.149E+19
6	2	75.0	0.1500	1.886E+19	4.317	8.141E+19
7	3	77.9	0.2500	2.791E+19	4.356	1.216E+20
8	4	81.9	0.3500	4.679E+19	4.406	2.061E+20
9	5	84.8	0.4500	6.704E+19	4.441	2.977E+20
10	6	87.9	0.5500	9.643E+19	4.476	4.316E+20
11	7	89.0	0.6500	1.096E+20	4.489	4.918E+20
12	8	91.9	0.7500	1.520E+20	4.520	6.873E+20
13	9	92.9	0.8500	1.711E+20	4.532	7.756E+20
14	10	101.1	0.9500	4.068E+20	4.616	1.878E+21
15			sum =	1.102E+21	44.344	4.992E+21
16	n =	10				
17	m =	10.28001	←Guess m in cell B17 and solve for maximum			
18			likelihood value of m to make sum in cell D22 = 0			

$$\frac{\sum_{i=1}^{n}\sigma_i^m\ln(\sigma_i)}{\sum_{i=1}^{n}\sigma_i^m} - \frac{1}{n}\sum_{i=1}^{n}\ln(\sigma_i) - \frac{1}{m} = 0 \quad \text{(A)}$$

22		Sum of terms in Eq. (A) =		3.64986E-14		

$$\sigma_\theta = \left[\frac{1}{n}\sum_{i=1}^{n}(\sigma_i^m)\right]^{1/m} = \quad 89.0 \quad \text{(B)}$$

FIGURE 5. Excel Spreadsheet After Solver Has Found $m = 10.28$ for the Weibull Modulus in Cell B17 to Make the Sum in Cell D22 Zero.

TABLE 1. Unbiasing Factor for Weibull Modulus From ASTM C1239.

Number of Test Specimens, n	Unbiasing Factor	Number of Test Specimens, n	Unbiasing Factor
5	0.700	26	0.947
6	0.752	28	0.951
7	0.792	30	0.955
8	0.820	32	0.958
9	0.842	34	0.960
10	0.859	36	0.962
11	0.872	38	0.964
12	0.883	40	0.966
13	0.893	42	0.968
14	0.901	50	0.973
15	0.908	60	0.978
16	0.914	70	0.981
18	0.923	80	0.984
20	0.931	90	0.986
22	0.938	100	0.987
24	0.943	120	0.990

WEIBULL SCALE PARAMETER σ_o

From measured strengths listed in Figure 4, we used the maximum likelihood method to find the unbiased Weibull modulus $m_{unbiased}$ and the characteristic strength σ_θ. Henceforth, we will delete the subscript in $m_{unbiased}$ and assume that you have found the unbiased Weibull modulus, which we will just call m.

Our job now is to find the Weibull scale factor σ_o for Equation 2, in which the effective area A_e of a specimen is taken into account. The factor A_o in Equation 2 is one unit of area, such as 1 cm^2, so that the exponent is dimensionless.

Weibull equation with Weibull scale parameter σ_o

$$P_f = 1 - e^{-\left(\frac{A_e}{A_o}\right)\left(\frac{\sigma}{\sigma_o}\right)^m}$$

(2)

Test specimens for Figures 1 and 2 are disks with a radius of 1.9 cm and a thickness of 0.020 cm tested in ring-on-ring fixture with a load radius of 0.80 cm and support radius of 1.60 cm. Equation 6 gave the effective area of the specimen:

Effective area for ring-on-ring test
$$A_e = 2\pi a^2 \left\{ 1 + \frac{44(1+\nu)}{3(1+m)} \frac{5+m}{2+m} \left(\frac{b-a}{bc}\right)^2 \left[\frac{2c^2(1+\nu)+(b-a)^2(1-\nu)}{(3+\nu)(1+3\nu)}\right] \right\} \quad (6)$$

where a is the load radius, b is the support radius, c, is the disk radius, m is the unbiased Weibull modulus (8.83), and ν is Poisson's ratio (0.30). Therefore, the effective area is

$$A_e = 2\pi(0.80)^2 \left\{ 1 + \frac{44(1+0.30)}{3(1+8.83)} \frac{5+8.83}{2+8.83} \left(\frac{1.6\text{-}0.8}{(1.6)(1.9)}\right)^2 \left[\frac{2(1.9)^2(1+0.30)+(1.6\text{-}0.8)^2(1\text{-}0.30)}{(3+0.30)(1+3[0.30])}\right] \right\}$$

$$A_e = 5.10 \text{ cm}^2.$$

Now we can find the Weibull scale parameter σ_o with Equation 3:

$$\sigma_o = \sigma_\theta \left(\frac{A_e}{A_o}\right)^{1/m} = (89.0 \text{ MPa}) \left(\frac{5.10 \text{ cm}^2}{1 \text{ cm}^2}\right)^{\frac{1}{8.83}} = 107.0 \text{ MPa} \quad (3)$$

With $\sigma_o = 107.0$ MPa in Equation 2, we can predict the cumulative probability of failure for any particular effective area in tension. Recall that σ_o is the Weibull characteristic strength if the effective area of the specimen is 1 cm^2.

Example: Expected mean strength. Calculate the expected mean strength for the 10 samples listed in Figure 4. The observed mean is 84.9 MPa.

To find the expected mean strength, substitute $\sigma_o = 107.0$ MPa, $A_e = 5.10 \text{ cm}^2$, and $m = 8.83$ into Equation 4:

$$\text{Expected mean strength} = \sigma_o \left(\frac{A_o}{A_e}\right)^{1/m} \Gamma\left(1 + \frac{1}{m}\right) \quad (4)$$

$$= (107.0 \text{ MPa}) \left(\frac{1 \text{ cm}^2}{5.10 \text{ cm}^2}\right)^{\frac{1}{8.83}} \Gamma\left(1 + \frac{1}{8.83}\right) = 84.2 \text{ MPa}$$

in which the gamma function is evaluated with the Excel statement =exp(gammaln(1+1/8.83)), giving $\Gamma = 0.946$. The predicted mean of 84.2 MPa is close to the observed value of 84.9 MPa. We just confirmed the plausibility of Equation 4 for the expected mean strength of a set of samples with effective area A_e and Weibull parameters m and σ_o.

STRENGTH SCALES WITH AREA UNDER STRESS

The larger the area of a ceramic, the lower the strength because the probability of finding a large flaw is greater in a large area. A slightly rewritten form of Equation 3 relates the expected mean strength S_2 for specimens with effective area A_2 to the observed mean strength S_1 for specimens with effective area A_1.

Weibull area scaling
$$\frac{S_2}{S_1} = \left(\frac{A_1}{A_2}\right)^{1/m}.$$
(13)

If a material fails from flaws distributed throughout its volume, we would replace areas in Equation 13 with volumes. To derive Equation 13, substitute S_2 for σ_o, S_1 for σ_θ, A_1 for A_e, and A_2 for A_o in Equation 3.

Example: Predicting flexure strength for components with different size. Disks for Figure 1 with an effective area of 5.10 cm² have an observed mean strength $S_1 = 84.9$ MPa with a Weibull modulus of $m = 8.83$ and Weibull scale factor of $\sigma_o = 107.0$ MPa. Use Equation 4 to predict the mean strength of the same quality of material with an effective area of 200 cm² under tensile stress. Substituting Weibull parameters into Equation 4 gives the prediction:

$$\text{Expected mean strength} = \sigma_o \left(\frac{A_o}{A_e}\right)^{1/m} \Gamma\left(1 + \frac{1}{m}\right)$$
(4)

$$= (107.0 \text{ MPa}) \left(\frac{1 \text{ cm}^2}{200 \text{ cm}^2}\right)^{\frac{1}{8.83}} \Gamma\left(1 + \frac{1}{8.83}\right) = (107.0 \text{ MPa})(0.5488)(0.9461) = 55.6 \text{ MPa}$$

We predict that the 200-cm² specimens will fail at a mean stress of 55.6 MPa. The greater the Weibull modulus, the less the strength depends on area. For $m = 15$, we would predict that the mean strength of the 200-cm² specimens would be 72.6 MPa.

EXPERIMENTAL CONFIRMATION OF WEIBULL AREA SCALING

Figure 6 shows experimental data that conform to the Weibull scaling law in Equation 13 for areas varying over a factor of 130. Taking the base 10 logarithm of both sides of Equation 13 gives

$$\log S_2 = -\frac{1}{m} \log\left(\frac{A_2}{A_1}\right) + \log S_1$$
(14)

We can measure the mean strengths (S_2) of sets of samples with a different effective area (A_2) for each set. Taking $A_1 = 1$ cm^2, Equation 14 predicts that a graph of $\log S_2$ versus $\log A_2/A_1$ will be a straight line with a slope of $-1/m$ and a y-intercept of $\log S_1$ when $\log A_2/A_1 = 0$ (that is, when $A_2 = 1$ cm^2). From the least-squares slope in Figure 6, $m = -1/(-0.0640) = 15.6$.[*] From the intercept in Figure 6, the predicted strength for an area of 1 cm^2 is $10^{2.4809} = 303$ MPa.
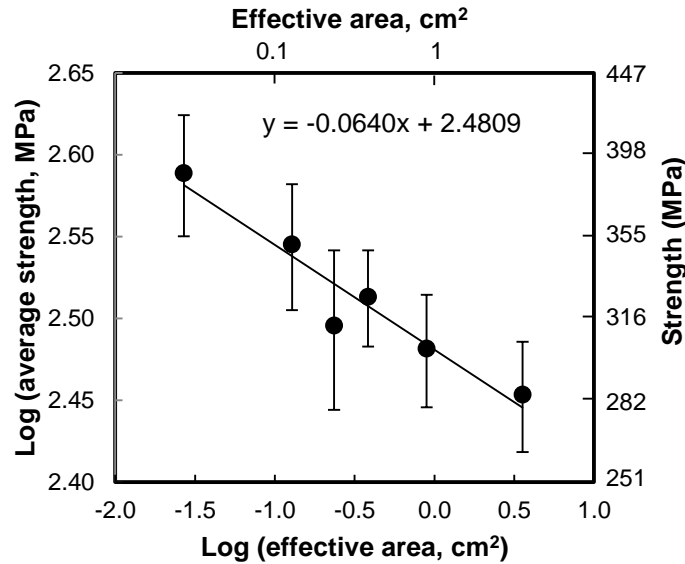
Test and Sample Type*	Number of Specimens	Effective Area, cm^2	Average Strength, MPa	Standard Deviation, MPa	Weibull Modulus for Set
3-point bend	18	0.0269	388	33	14.6
4-point bend	17	0.235	313	35	9.4
3-point bend	18	0.128	351	31	12.2
4-point bend	48	0.894	303	24	14.3
3-point bend	18	0.384	326	22	16.4
4-point bend	18	3.57	284	22	14.5

FIGURE 6. Demonstration of Weibull Area Scaling for Sintered Silicon Carbide 3- and 4-Point Flexure Bars. Data from C. A. Johnson and W. T. Tucker in ASTM C1683-10 (Reference 7). Error bars are ±one standard deviation.

---

[*]ASTM C1683-10 gives Weibull modulus = -1/slope = 14.4 for the data in Figure 6. The ASTM document does not list the effective areas of the six types of samples. We computed the effective areas listed in Figure 6, producing a slope of -0.0640 and a Weibull modulus of 15.6. It is possible that ASTM C1683-10 had different effective areas from what we used. It is also possible that ASTM C1683-10 found the Weibull modulus of 15.6, but then applied an unbiasing factor 0f 0.923 for 18 data points, reducing the Weibull modulus to (0.923)(15.6) =14.4.

**COMPILATION OF WEIBULL PARAMETERS
FOR INFRARED WINDOW MATERIALS**

Table 2 lists the Weibull modulus *m* and Weibull scale factor σ_o derived by ASTM C1239 maximum likelihood analysis of mechanical test data for infrared window materials. Each data set must include the test fixture size so that effective area can be calculated.

The last two columns of Table 2 give expected mean strength computed with Equation 4 for effective areas of $A_e = 10 \text{ cm}^2$ and 500 cm^2. The area of 10 cm^2 corresponds roughly to a 2-inch-diameter circular window in Figure 3 and 500 cm^2 corresponds roughly to a 16-inch-diameter circular window.

Weibull scaling with Equation 13 states how the strength decreases as effective area in tension increases. The lower the Weibull modulus, the more rapidly strength decreases with increasing area. Consider aluminum oxynitride (ALON) and fused quartz, both with a conventional finish in Table 2. For $A_e = 10 \text{ cm}^2$, the expected means strengths are ~225–250 MPa for ALON and ~90–110 MPa for fused quartz. ALON is the stronger of the two materials. But for $A_e = 500 \text{ cm}^2$, the expected means strengths are ~60–75 MPa for ALON and ~60–75 MPa for fused quartz. The two materials are predicted to have equal strengths in a 16-inch-diameter window because the Weibull modulus of fused quartz ($m \approx 10$) is greater than the Weibull modulus of ALON ($m \approx 4$), so the strength of ALON falls off more rapidly with increasing area.

TABLE 2. Strengths of Infrared Window Materials: ASTM C1239 Weibull Parameters.

| Material | Temp, °C | ASTM C1239 Weibull Parameters | | Expected Mean Strength for Effective Area | |
		Unbiased m	σ_o, MPa	$A_e = 10$ cm^2 ~2-inch diameter	$A_e = 500$ cm^2 ~16-inch diameter
Aluminum oxynitride, $9Al_2O_3 \cdot {\sim}3.6AlN$ (polycrystalline ALON)					
Manufacturer 1[a]	~20	4.3	328	175	70
Manufacturer 2 commercial finish[b]	~20	2.9	559	225	58
Manufacturer 2 commercial finish[b]	500	3.2	577	252	74
Manufacturer 2 extra care in finishing[b]	~20	4.1	828	429	165
Calcium fluoride, CaF_2					
Fusion cast polycrystalline CaF_2[c]	~20	3.1	111	47	13
Single crystal (111) CaF_2[d]	~20	2.8	83	32	8
Diamond (CVD, chemical vapor deposited thick film) (polycrystalline)					
Manufacturer 1 optical grade[e]	~20	7.4	442	304	179
Manufacturer 2[f]	~20	2.8	520	203	50
Fused quartz, SiO_2 (similar to fused silica) immersed in water					
25.4-mm-diameter disks[g]	20	10.8	120	93	64
76.2-mm-diameter disks[g]	20	11.0	135	105	73
228.6-mm-diameter disks[g]	20	7.4	162	111	66
25.4-mm-diam. disks, superpolished[g]	20	9.4	180	134	88
Germanium, Ge (polycrystalline)					
20.0-mm-diameter disks[h]	~20	4.4	179	97	40
76.2-mm-diameter disks[h]	~20	4.5	237	130	54
128-mm-diameter disks[ha]	20	5.6	341	222	104
51-mm-diameter disks[ha]	23	6.4	291	189	103
Magnesium fluoride, MgF_2 (polycrystalline)					
Hot pressed U.S. material from 1970s[i]	~20	4.4	218	118	48
Hot pressed French material from 1990s[j]	~20	3.3	190	85	26
Single crystal[k]	~20	~4.9	~160	~92	~41
Hot pressed U.S. material from 1970s[l]	24	8.4	113	81	51
	121	15	121	100	77
	260	10.8	120	93	64
	399	5.6	107	66	33
	538	4.9	86	49	22
Nanocomposite optical ceramic ($MgO{:}Y_2O_3$ 50:50 vol:vol)					
38-mm-diameter disks[m]	21	6.8	819	545	307
38-mm-diameter disks[n]	600	5.8	580	361	184
Polycrystalline alumina (Al_2O_3) (infrared-transparent material with grain size 0.3–0.4 μm)					
2008 data set[o]	24	6.3	1352	873	459
2016 data set[o]	21	11.8	867	683	490
2016 data set[o]	500	11.6	758	595	425
2016 data set[o]	750	11.9	715	564	406
2016 data set[o]	1000	10.3	672	512	350

TABLE 2. (Contd.)

Material	Temp, °C	ASTM C1239 Weibull Parameters		Expected Mean Strength for Effective Area	
		Unbiased m	σ_o, MPa	$A_e = 10\ cm^2$ ~2-inch diameter	$A_e = 500\ cm^2$ ~16-inch diameter
Sapphire (Al_2O_3) a-plane					
a-Plane HEM material as polished[p]	~20	6.1	752	479	252
a-Plane HEM material annealed[p]	~20	7.4	919	632	372
a-Plane HEM material[q]	~20	5.0	1426	826	378
a-Plane HEM material[q]	600	6.0	1052	692	383
a-Plane HEM material (no Grafoil®)[r]	~20	3.5	1170	545	178
a-Plane HEM material (no Grafoil®)[r]	800	2.2	1124	350	59
a-Plane HEM material[s]	~20	5.6	1072	657	327
a-Plane EFG material[t]	~20	4.2	1116	586	231
a-Plane EFG material[u]	~20	2.8	1373	537	133
Sapphire (Al_2O_3) c-plane					
c-Plane HEM material (with Grafoil®)[v]	~20	4.0	2778	1416	532
c-Plane HEM material (with Grafoil®)[v]	600	4.7	853	478	208
c-Plane HEM material (no Grafoil®)[w]	~20	2.5	2707	956	200
c-Plane HEM material (no Grafoil®)[w]	800	10.4	173	132	91
c-Plane HEM material[x]	~20	2.7	1840	697	164
c-Plane Czochralski material[y]	~20	2.7	1876	711	167
Sapphire (Al_2O_3) r-plane					
r-Plane HEM material[z]	~20	4.2	795	418	165
r-Plane Czochralski material[aa]	~20	3.5	923	430	141
Spinel ($MgAl_2O_4$) (polycrystalline)					
Coarse grain size (~200 μm)[ab]	~20	6.1	220	140	74
Coarse grain size (~200 μm)[ac]	~20	5.5	186	113	55
Coarse grain size (~200 μm)[ah]	~20	5.0	153	88	40
Coarse grain size (~200 μm)[ad]	~20	6.5	174	114	62
Coarse grain size (~200 μm) extra care in finish[ae]	~20	6.1	275	175	92
Coarse grain size (~200 μm)[af]	~20	4.6	377	209	89
Medium grain size (≲20 μm)[ag]	~20	4.7	390	219	95
Fine grain size (≲5 μm)[ah]	~20	6.6	649	427	236
Fine grain size (≲2 μm)[ai]	~20	8.7	501	364	232
Yttria (Y_2O_3) (polycrystalline)					
Yttria[aj]	~20	7.0	131	88	50
9 mol% lanthana-doped yttria[aj]	~20	6.3	194	125	67
Zinc selenide, ZnSe (CVD, chemical vapor deposited)					
CVD ZnSe[ak]	~20	16.6	60	51	40
CVD ZnSe[al]	~20	8.7	81	59	37
Zinc sulfide, ZnS (CVD, chemical vapor deposited standard grade)					
Standard grade[am]	~20	4.7	124	70	30
Standard grade[an]	~20	10.1	140	106	72
Standard grade 1988 data[ao]	21	6.9	100	67	38
	121	6.3	118	76	41
	260	5.9	144	90	47
	399	4.3	181	96	39
	538	4.1	216	112	43
	677	5.4	199	120	58

TABLE 2. (Contd.)

Material	Temp, °C	ASTM C1239 Weibull Parameters		Expected Mean Strength for Effective Area	
		Unbiased m	σ_o, MPa	$A_e = 10$ cm^2 ~2-inch diameter	$A_e = 500$ cm^2 ~16-inch diameter
Zinc sulfide, ZnS (CVD, chemical vapor deposited multispectral grade)					
Multispectral grade[ap]	~20	8.6	90	65	41
Multispectral grade[aq]	16	9.7	82	61	41
Multispectral grade[aq]	200	12.5	96	77	56

a. Fifteen ring-on-ring disks. Data points read from Reference 8.

b. Twenty-eight ring-on-ring disks with commercial finish tested at ~20°C. Thirty disks with commercial finish tested at 500°C. Twenty-one disks with extra care in finishing. Reference 9.

c. Thirty 4-point flexure bars. Data points read from Reference 10. Data originally from Reference 11. Reference 10 interpreted the fracture data in terms of a bimodal distribution of failures characterized by 46% with low strength and $m = 6.9$ and 54% with high strength and $m = 6.1$. Combination of the two modes produces similar behavior to one failure mode with $m \approx 3$ and intermediate strength.

d. Six 4-point flexure bars. Data points read from Reference 12. Data originally from Reference 13.

e. Optical quality CVD diamond 0.33 mm thick with growth surface in tension. Seventeen 20-mm-diameter disks tested in biaxial flexure by disk-burst method with 16-mm support diameter. Growth surface strength decreases as diamond gets thicker and crystallite size on the growth surface increases. Reference 14.

f. Multiple thicknesses (0.2–0.6 mm thick) of CVD diamond disks with 17–19 mm diameter tested in ring-on-ring flexure with nucleation surface in tension. The strength of the nucleation surface is nearly independent of thickness because the grain size on the nucleation surface is small and does not change as the film grows thicker. Load diameter = 7.0 mm and support diameter = 14.0 mm. Data points read from Reference 8.

g. Sets of 23–28 General Electric Type 124 fused quartz disks (4 mm thick) tested in ring-on–ring flexure at a load rate of 200 N/s with tensile surface immersed in distilled water. Large disks were all polished in an identical manner and smaller disks were laser cut from large disks. The "super polished" set of 11 disks had additional polish to reduce the size of residual flaws. Load and support diameters were (10.58, 21.16 mm), (28.58, 57.15 mm), (95.25, 190.5 mm), and (8.0, 16.0 mm) for the different size specimens. Small load/support diameters for super polished set were necessary to eliminate edge failure. Failures outside of the inner gauge section (the load ring) were rejected by the authors. Therefore, the effective area was taken as $A_e = 2\pi a^2$, where a = load ring radius. The factor of 2 accounts for hoop and radial stress components. Data from Reference 15.

h. Thirty ring-on-ring flexure disks tested with Delrin load and support rings to reduce contact stress. Small disks 2.01 mm thick were tested with 8.74 mm load diameter and 17.94 mm support diameter. Large disks 6.21 mm thick were tested with 31.75 mm load diameter and 63.50 mm support diameter. Outer gauge section failures included in Weibull analysis. Data points read from Reference 16.

ha. Polished ring-on-ring disks with measured Poisson's ratio = 0.22. Set of 18 disks with thickness 3.21 mm, diameter 51.27 mm, support diameter 39.82 mm, load diameter 19.89 mm. Set of 26 disks with thickness 8.54 mm, diameter 128.16 mm, support diameter 101.6 mm, load diameter 50.8 mm. Data provided by J. Salem from Reference 17.

i. Fifteen ring-on-ring disks. Reference 18.

j. Thirty ring-on-ring disks measured by W. F. Adler with Delrin rings.

k. Three sets of 19–21 ring-on-ring disks with three different polishing procedures. Reference 19.

l. Four-point flexure bars; length = 25.4 mm, thickness = width = 1.78 mm, load span = 8.38 mm, support span = 16.76 mm. Number of specimens at each temperature: 24°C, $n = 20$; 121°C, $n = 9$; 260°C, $n = 15$; 399°C, $n = 18$; 538°C, $n = 16$.

m. Fourteen ring-on-ring disks. Reference 20.

n. Sixteen ring-on-ring disks. Reference 20. Weibull parameters in the table are derived by omitting the two strongest specimens from 18 disks tested. If all 18 results are used, derived parameters are $m = 3.6$ and $\sigma_o = 700$ MPa, giving predicted strengths of 333 and 184 MPa for $A_e = 10$ and 500 cm^2, respectively. Discarding the two strongest samples increases the apparent Weibull modulus and predicts greater strength for large windows.

o. Twenty-three to 30 ring-on-ring disks. References 21, 22, and 23.

p. HEM = heat exchanger method. Fourteen ring-on-ring disks. Reference 24. Annealing conditions are not stated, but it has been shown that annealing near 1200°C in air strengthens sapphire by healing some polishing damage (Reference 25).

q. HEM = heat exchanger method. Ten ring-on-ring disk. Reference 26.

r. HEM = heat exchanger method. No Grafoil® was used between specimen and test fixture. Twenty ring-on-ring disks at ~20°C and 22 disks at 800°C. References 27 and 28.

s. HEM = heat exchanger method. Eleven ring-on-ring disks.

t. EFG = edge-defined film-fed growth method. Nine ring-on-ring disks.

u. EFG = edge-defined film-fed growth method. Twenty six ring-on-ring disks.

v. HEM = heat exchanger method. Eight ring-on-ring disks at ~20°C and 11 disks at 600°C. Reference 26.

w. HEM = heat exchanger method. No Grafoil® was used between specimen and test fixture. Twenty ring-on-ring disks at ~20°C and at 800°C. References 27 and 28.

x. HEM = heat exchanger method. Eight ring-on-ring disks. Data points read from Reference 8.

y. Czochralski crystal growth. Eight ring-on-ring disk. Data points read from Reference 8.

z. HEM = heat exchanger method. Twelve ring-on-ring disks. Data points read from Reference 8.

aa. Czochralski crystal growth. Six ring-on-ring disks. Data points read from Reference 8.

ab. Ten ring-on-ring disk taken from 23-mm-thick plate.

ac. Twenty-three ring-on-ring disks taken from a large plate.

ad. Fourteen ring-on-ring disks taken from a large plate.

ae. Twenty-one ring-on-ring disks taken from a large plate.

af. Twenty-seven ring-on-ring disks taken from a large plate.

ag. Fifteen ring-on-ring disks.

ah. Fifteen ring-on-ring disks.

ai. Seventeen ring-on-ring disks. From Reference 29. Data courtesy S. Sweeney.

aj. Materials produced in 1987. Forty ring-on-ring disks. References 30, 31, and 32.

ak. Twenty ring-on-ring disks. Data points read from Reference 8.

al. Fifteen ring-on-ring disks tested in distilled water at 10.2 MPa/s. Data from Reference 33.

am. Thirteen ring-on-ring disks.

an. Twenty ring-on-ring disks. Data points read Reference 8.

ao. Twenty ring-on-ring disks. Data from Reference 34.

ap. Twenty ring-on-ring disks. Data points read from Reference 8.

aq. ASTM C1161Size C 4-point flexure bars: 24 bars at 16°C and 23 bars at 200°C. Reference 35.

WEIBULL PROBABILITY OF SURVIVAL WITHOUT
SLOW CRACK GROWTH

How can we use the Weibull equation to predict the probability of survival of a window made from a material whose strength we have measured with coupons? Consider the transparent polycrystalline alumina window in Figure 7 held in a frame by a compliant gasket with a pressure difference $P = 0.5$ MPa (5 bar) across the window. The right side of the window becomes convex and is placed in tension. The maximum stress at the center of the tensile face computed with Equations 15 and 16 (Reference 4) is 364.8 MPa. Poisson's ratio and Young's modulus given in the figure caption apply to a fine-grain polycrystalline alumina (grain size 0.3–0.4 μm) that is transparent in the midwave infrared region and visibly translucent (References 22, 36 through 40).
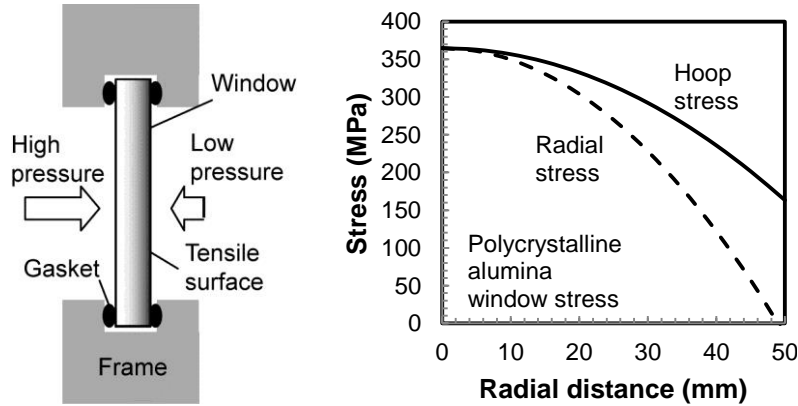

FIGURE 7. Window in a Frame With Pressure Difference $P = 0.5$ MPa Across the Window. Window radius $c = 55$ mm, support radius (gasket radius) $b = 50$ mm, window thickness $d = 2.0$ mm, Poisson's ratio $\nu = 0.24$, and Young's modulus $E = 403$ GPa.

$$\text{Radial stress} = \frac{3Pb^2}{8d^2}\left[(1-\nu)\left(\frac{b^2}{c^2}\right) + 2(1+\nu) - (3+\nu)\left(\frac{r^2}{b^2}\right)\right] + \frac{(3+\nu)P}{4(1-\nu)} \qquad (15)$$

$$\text{Hoop stress} = \frac{3Pb^2}{8d^2}\left[(1-\nu)\left(\frac{b^2}{c^2}\right) + 2(1+\nu) - (1+3\nu)\left(\frac{r^2}{b^2}\right)\right] + \frac{(3+\nu)P}{4(1-\nu)} \qquad (16)$$

where r is the radial location measured from the center of the window, b is the radius of the gasket ring (Figure 3), c is disk radius, d is disk thickness, ν is Poisson's ratio, and P is the pressure difference between the two surfaces.

Figure 8 shows the strengths of 25 coupons of polycrystalline alumina tested in ambient atmosphere in ring-on-ring flexure. Experiments that are not shown suggest that slow crack growth in polycrystalline alumina at ambient humidity near room temperature is negligible. Weibull analysis by the maximum likelihood method gives an unbiased Weibull modulus of $m = 11.8$ and a Weibull scale factor of $\sigma_o = 867$ MPa.
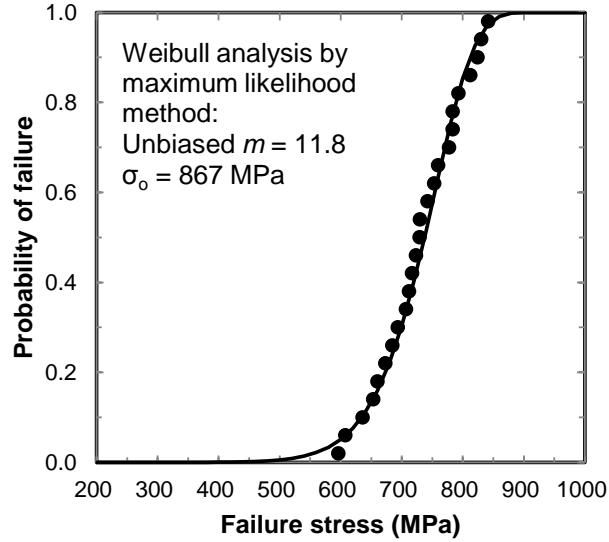

FIGURE 8. Weibull Plot of Strengths of 25 Transparent Polycrystalline Alumina Disks With Radius 1.90 cm and Thickness 0.203 cm Using a Ring-on-Ring Test Fixture With Load Radius 0.794 cm and Support Radius 1.588 cm Tested in Air at 20% Relative Humidity at 21°C With Crosshead Speed 0.508 mm/min. CeraNova data.

Weibull Equation 2 gives the probability of failure P_f as a function of applied stress σ and effective area A_e in tension. The probability of survival P_s is $1 - P_f$:

$$\text{Weibull probability} \atop \text{of survival} \qquad P_s = 1 - P_f = e^{-\left(\frac{A_e}{A_0}\right)\left(\frac{\sigma}{\sigma_0}\right)^m} \tag{17}$$

Equation 17 is the key to static Weibull analysis to evaluate the probability of survival in the absence of slow crack growth.

For the window in Figure 7, Equation 7 gives the effective area:

$$A_e \approx \frac{4\pi(1+v)}{1+m}\left(\frac{b}{c}\right)^2\left[\frac{2c^2(1+v)+b^2(1-v)}{(3+v)(1+3v)}\right] \tag{7}$$

$$A_e \approx \frac{4\pi(1+0.24)}{1+11.8}\left(\frac{5.0}{5.5}\right)^2\left[\frac{2*5.5^2(1+0.24)+5.0^2(1-0.24)}{(3+0.24)(1+3*0.24)}\right] = 16.97 \text{ cm}^2$$

Substituting $A_e = 16.97\ \text{cm}^2$ into Equation 17 predicts the probability of survival:

$$P_s = e^{-\left(\frac{A_e}{A_o}\right)\left(\frac{\sigma}{\sigma_o}\right)^m} = e^{-\left(\frac{16.97\ \text{cm}^2}{1\ \text{cm}^2}\right)\left(\frac{364.8\ \text{MPa}}{867\ \text{MPa}}\right)^{11.8}} = 0.999380 \qquad (18)$$

The window has a 99.94% probability of survival or a probability of failure of $P_f = 1 - P_s = 1 - 0.9994 = 0.06\%$.

For some purposes, we desire a lower probability of failure. We can decrease the probability of failure by reducing tensile stress with a thicker window. Different values of thickness in Equation 15 give the following stresses and probabilities of failure:

Thickness d, mm	Maximum Stress, MPa	Probability of Failure P_f
1.5	648.1	0.42
1.75	476.3	0.014
2.0	364.8	0.0006
2.25	288.3	0.00004
2.5	233.6	0.000003

Window thickness is the principal handle available for obtaining an acceptable probability of failure.

GENERAL APPROACH TO WEIBULL PROBABILITY OF SURVIVAL

In the previous section, we used the effective area of the window to compute the probability of survival with Equation 17. In many situations, we do not have closed-form equations for stress or effective area. Commonly, a finite element analysis produces a map of the principal stresses in each element of surface area (or volume) of a window or dome that might have a complex shape.

Figure 9 shows the circular window in Figure 8 divided into a 10 annular regions inside the support radius from a radial distance $r = 0$ to $r = 50$ mm. A more complex shape could be divided into smaller elements of arbitrary shape. The principal surface stresses for a circular window are the hoop and radial stresses. We will compute the Weibull probability of survival of each annulus and then find the probability of survival of the entire window as the product of probabilities of survival of all the annuli.
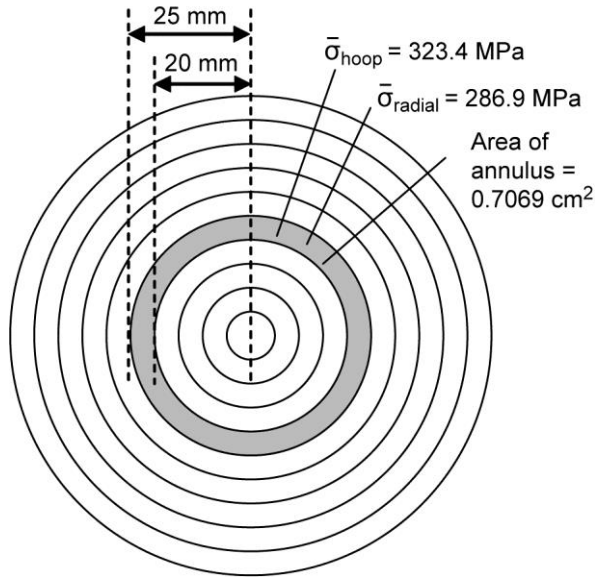
FIGURE 9. Computing Weibull Probability of Survival by Dividing a Window Into Many Surface Elements and Computing the Probability of Survival of Each Element. Overall probability of survival is the product of probabilities of survival for each element.

Consider the shaded annulus extending from $r_1 = 20$ to $r_2 = 25$ mm. The geometric area of the annulus is $A = \pi r_2^2 - \pi r_1^2 = 0.7069$ cm^2. Table 3 lists the following stresses computed with Equation 16:

Hoop stress at r = 20 mm: 332.5 MPa ⎱ Average hoop stress =
Hoop stress at r = 25 mm: 314.4 MPa ⎰ $\frac{1}{2}(332.5 + 314.4) = 323.4$ MPa

Table 3 shows the average radial stress in the same annulus to be 286.9 MPa.

The probability of survival of the annulus is the product of the Weibull probabilities of survival from the hoop and radial stresses computed from the geometric area of the annulus with Equation 17:

$$P_s(\text{hoop}) = e^{-\left(\frac{A_e}{A_o}\right)\left(\frac{\sigma}{\sigma_o}\right)^m} = e^{-\left(\frac{0.7069 \text{ cm}^2}{1 \text{ cm}^2}\right)\left(\frac{323.4 \text{ MPa}}{867 \text{ MPa}}\right)^{11.8}} = 0.999937$$

$$P_s(\text{radial}) = e^{-\left(\frac{A_e}{A_o}\right)\left(\frac{\sigma}{\sigma_o}\right)^m} = e^{-\left(\frac{0.7069 \text{ cm}^2}{1 \text{ cm}^2}\right)\left(\frac{286.9 \text{ MPa}}{1352 \text{ MPa}}\right)^{11.8}} = 0.999985$$

$$P_s(annulus) = P_s(hoop) \times P_s(radial) = (0.999937)(0.999985) = 0.999922$$

The probability of survival of the shaded annulus is 0.999922.

TABLE 3. Weibull Probability of Survival of a Window Found
From the Stress in Each Element of Area.

Radial Distance, mm	Hoop Stress, MPa	Radial Stress, MPa	Annular Area, mm^2	Mean Hoop Stress, MPa	Hoop Probability of Survival P_s	Mean Radial Stress, MPa	Radial Probability of Survival P_s
0	364.8	364.8	---	---	---	---	---
5	362.7	361.0	78.5	363.8	0.999972	362.9	0.999973
10	356.7	349.6	235.6	359.7	0.999927	355.3	0.999937
15	346.6	330.6	392.7	351.7	0.999907	340.1	0.999937
20	332.5	304.0	549.8	339.6	0.999914	317.3	0.999961
25	314.4	269.8	706.9	323.4	0.999937	286.9	0.999985
30	292.2	228.1	863.9	303.3	0.999964	249.0	0.999997
35	266.0	178.7	1021.0	279.1	0.999984	203.4	1.000000
40	235.8	121.8	1178.1	250.9	0.999995	150.2	1.000000
45	201.5	57.2	1335.2	218.6	0.999999	89.5	1.000000
50	163.2	-14.9	1492.3	182.3	1.000000	21.1	1.000000

The probability of survival of the entire window is the product of probabilities of survival of all 10 annuli, which is

$$P_s(\text{window}) =$$
$$\underbrace{(0.999972)(0.999973)}_{P_s(\text{annulus 1})} \times \underbrace{(0.999927)(0.999937)}_{P_s(\text{annulus 2})} \dots \underbrace{(1.000000)(1.000000)}_{P_s(\text{annulus 10})} = 0.999388 \qquad (19)$$

This approximate method of breaking the window into multiple small areas gives us an estimate of $P_s = 0.999388$ for the overall probability of survival of the window. We found the value $P_s = 0.999380$ for the window with Equation 18 from the effective area of the entire window. In general, there would be some difference in P_s found by the two methods. The fidelity of the approximate method is improved by breaking the object into more small elements.

To recap, the general method for finding Weibull probability of survival is to divide the window into small elements and compute the principal tensile stresses in each surface element by finite element analysis. Then find the probability of survival of each surface element with Equation 17 using the geometric area for each element and the mean principal stresses in that element. The overall probability of survival is the product of probabilities of survival of all the surface elements.

SOME CAVEATS FOR WINDOW DESIGN

The procedure in the last two sections assumes that the window has the same flaw distribution (and therefore Weibull parameters) as the test coupons used to measure Weibull parameters. A similar statement might be that the coupons are ground and polished by the same methods used to make the window. Even if machining of coupons is matched as well as possible to that of the window, it is not reasonable to expect flaw populations to be exactly the same. Anecdotal evidence suggests that every time the same nominal procedure is used in one shop to finish the same kinds of samples, mechanical strength test results are different. One of many possible reasons for differing results is that the condition of the abrasive used for grinding and polishing changes during use of the abrasive, so the abrasive is never the same from run to run.

Another caveat is that Weibull area scaling works best if the stress state of the window is similar to the stress state of the test coupons. We chose an example in which the window is in a "pressure-on-ring" stress state and the test coupons are in a "ring-on-ring" stress state, which are approximately similar conditions. The more the window stress state differs from the coupon stress state, the less likely are predictions of probability of survival to be meaningful.

One procedure used by designers is to calculate the 90% upper and lower confidence limits for the Weibull parameters by using equations given in ASTM C1239. Window performance can then be calculated with the upper and lower bound Weibull parameters to see what range of predictions results.

The two parameter Weibull Equation 1 gives more conservative predictions of survival than a three parameter equation in which there is a lower stress limit below which the probability of failure is considered to be zero.

Ultimately, it is excellent practice to proof test real windows to verify at some level of confidence that a manufactured window withstands its design conditions with some additional margin of safety.

MAXIMUM LIKELIHOOD METHOD

For the Weibull cumulative probability of failure function Equation 1,

Weibull equation with characteristic strength σ_θ

$$P_{\mathrm{f}} = 1 - \mathrm{e}^{-\left(\frac{\sigma}{\sigma_\theta}\right)^m} \tag{1}$$

the *probability density p* is the derivative $dP_{\mathrm{f}}/d\sigma$:

Probability density

$$p \equiv \frac{dP_{\mathrm{f}}}{d\sigma} = \left(\frac{m}{\sigma_\theta}\right)\left(\frac{\sigma}{\sigma_\theta}\right)^{m-1} \mathrm{e}^{-\left(\frac{\sigma}{\sigma_\theta}\right)^m} \tag{20}$$

Unlike a Gaussian probability curve, Weibull probability is not symmetric about the peak. The maximum probability density of 0.00434 occurs at a stress of 542 MPa in Figure 10, whereas 50% cumulative probability of failure occurs at 530 MPa.
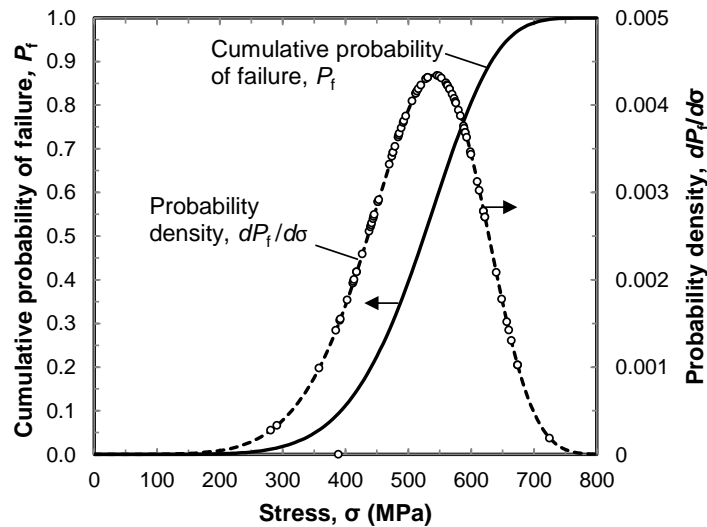

FIGURE 10. Weibull Cumulative Probability of Failure P_{f} From Equation 1 and Probability Density From Equation 20 for $m = 6.48$ and $\sigma_\theta = 555.8$ MPa. Open circles are experimental data for 80 4-point flexure specimens of hot isostatically pressed silicon carbide from Table 4 of ASTM C1239-13.

The experimental probability density for 80 flexure test specimens in Figure 10 conforms well to the dashed curve, which is the derivative of the solid line. Weibull parameters were found by the maximum likelihood method of ASTM C1239. The likelihood of observing experimental points is greatest at the peak of the probability density function.

The *likelihood function*, $\mathcal{L}$, for *n* experimental data points is the product of probability densities in Equation 20 for all points in the set of strength measurements:

Liklihood function
$$\mathcal{L} = \prod_{i=1}^{n} p_i = \prod_{i=1}^{n} \left(\frac{m}{\sigma_\theta}\right)\left(\frac{\sigma_i}{\sigma_\theta}\right)^{m-1} e^{-\left(\frac{\sigma_i}{\sigma_\theta}\right)^m} \tag{21}$$

where the symbol Π stands for a product just as Σ stands for a sum. Units of the likelihood function are 1/MPa, which means probability per megapascal.

Example: Maximum likelihood function. The spreadsheet in Figure 4 lists flexure strengths of 10 specimens. Write the first two terms of the likelihood function using trial Weibull parameters $m = 6$ and $\sigma_\theta = 87.3$ MPa found in cells B17 and D24 of the spreadsheet.

The first two measured strengths are 66.1 and 75.0 MPa, so the first two terms of the likelihood product are

$$\mathcal{L} = \prod_{i=1}^{n} \left(\frac{m}{\sigma_\theta}\right)\left(\frac{\sigma_i}{\sigma_\theta}\right)^{m-1} e^{-\left(\frac{\sigma_i}{\sigma_\theta}\right)^m} =$$
$$\left[\left(\frac{6}{87.3 \text{ MPa}}\right)\left(\frac{66.1 \text{ MPa}}{87.3 \text{ MPa}}\right)^{6-1} e^{-\left(\frac{66.1 \text{ MPa}}{87.3 \text{ MPa}}\right)^6}\right]\left[\left(\frac{6}{87.3 \text{ MPa}}\right)\left(\frac{75.0 \text{ MPa}}{87.3 \text{ MPa}}\right)^{6-1} e^{-\left(\frac{75.0 \text{ MPa}}{87.3 \text{ MPa}}\right)^6}\right]$$

There would be 10 terms in the likelihood product.

The maximum likelihood method seeks values of m and σ_θ that maximize the likelihood function in Equation 21. With trial values $m = 6$ and $\sigma_\theta = 87.3$ MPa, the product of all 10 terms in the example above is $\mathcal{L} = 1.832 \times 10^{-17}$ (MPa)$^{-1}$. The optimum values $m = 10.280$ and $\sigma_\theta = 89.05$ MPa derived in Figure 5 give the maximum likelihood $\mathcal{L} = 11.863 \times 10^{-17}$ (MPa)$^{-1}$.

To find the optimum values of m and σ_θ, recall that the derivative of a function is 0 at the maximum value of the function. Optimum values of m and σ_θ giving the maximum value of $\mathcal{L}$ must satisfy two simultaneous partial derivative equations of $\mathcal{L}$ with respect to m and σ_θ:

$$\frac{\partial \mathcal{L}}{\partial m} = 0 \quad \text{and} \quad \frac{\partial \mathcal{L}}{\partial \sigma_\theta} = 0 \tag{22}$$

It is inconvenient to write expressions for $\partial\mathcal{L}/\partial m$ and $\partial\mathcal{L}/\partial\sigma_\theta$ in Equation 22. However, values of m and σ_θ that maximize $\mathcal{L}$ also maximize the natural logarithm of $\mathcal{L}$ because $\ln \mathcal{L}$ increases monotonically as $\mathcal{L}$ increases.

To find the natural logarithm of $\mathcal{L}$, use the identity $\ln abc \ldots . = \ln a + \ln b + \ln c \ldots$. Applying this identity to the product of n terms in Equation 21, we can write a sum instead of a product:

$$\ln \mathcal{L} = \ln p_1 p_2 \cdots p_n = \ln p_1 + \ln p_2 + \cdots + \ln p_n$$

$$= \ln\left[\left(\frac{m}{\sigma_\theta}\right)\left(\frac{\sigma_1}{\sigma_\theta}\right)^{m-1} e^{-\left(\frac{\sigma_1}{\sigma_\theta}\right)^m}\right] + \cdots + \ln\left[\left(\frac{m}{\sigma_\theta}\right)\left(\frac{\sigma_n}{\sigma_\theta}\right)^{m-1} e^{-\left(\frac{\sigma_n}{\sigma_\theta}\right)^m}\right] \tag{23}$$

Taking derivatives with care, the two equations $\partial \ln \mathcal{L}/\partial m = 0$ and $\partial \ln \mathcal{L}/\partial \sigma_\theta = 0$ applied to Equation 23 produce Equations 9 and 10. We solved these equations with the spreadsheet in Figure 5 to find the maximum likelihood values of m and σ_θ.

SUMMARY

The most useful form of the Weibull equation for the cumulative probability of failure for materials that fail from surface flaws is Equation 2: $P_f = 1 - e^{-\left(\frac{A_e}{A_o}\right)\left(\frac{\sigma}{\sigma_o}\right)^m}$, in which m is the Weibull modulus. The Weibull scale factor, σ_o, is ideally a material property. The effective area in tension, A_e, is not equal to the geometric area in tension. Effective area is given for the ring-on-ring test configuration by Equation 6 and for the pressure on ring configuration by Equation 7. The reference area A_o is chosen as 1 cm^2 to cancel the units of A_e. The phenomenological Weibull Equation 1 $P_f = 1 - e^{-\left(\frac{\sigma}{\sigma_\theta}\right)^m}$ is written in terms of σ_θ, the Weibull characteristic strength, and does not include A_e. Equation 1 is transformed into Equation 2 with the substitution $\sigma_o = \sigma_\theta \left(\frac{A_e}{A_o}\right)^{1/m}$. The parameter σ_θ is not a material property.

Weibull parameters for a set of measured flexure strengths are derived by the maximum likelihood method according to ASTM C1239. Observed strengths are ordered from weakest to strongest in column B of Figure 4 and the observed probability of failure for each result is computed in column C with Equation 8. A Weibull modulus is guessed in cell B17 of Figure 4 in order to compute the terms in columns D, E, and F, whose sums are found in row 15. These sums are substituted into the maximum likelihood Equation 9. Then m is varied with Excel Solver to find the best value of m that minimizes the sum in Equation 9 in cell D22. The characteristic strength is computed with Equation 10 in cell D24. For a set of n strength measurements, the value of m is then reduced by multiplication by the unbiasing factor in Table 1. The Weibull scale factor σ_o is then computed from σ_θ with the effective area and unbiased value of m by using Equation 3.

Experimental values of unbiased *m* and σ_o for many infrared window materials are listed in Table 2. The last two columns of Table 2 use Equation 4 to predict the expected mean strengths of windows with a pressure-on-ring geometry (Figure 3) and effective areas in tension of 10 and 500 cm^2. Predicted strengths fall markedly with increased window area. The smaller the Weibull modulus, the more rapidly strength diminishes with increasing area under stress.

The static Weibull probability of survival of a window subjected to an applied pressure is computed by ignoring the possibility of slow crack growth under load. Equation 17 can be employed to calculate the probability of failure for a known effective area in tension. The stress σ in Equation 17 is the maximum stress on the tensile face of the window. Alternatively, a complex window shape is conceptually divided into small sections in Figure 9 and the probability of survival is computed for each component of tensile stress in each section. The overall probability of survival of the window is the product of probabilities of survival of each section.

REFERENCES

1. W. Weibull. "A Statistical Distribution Function of Wide Applicability," *J. Appl. Mech.*, Vol. 13, (1951), pp. 293–297.

2. ASTM International. "Standard Practice for Reporting Uniaxial Strength Data and Estimating Weibull Distribution Parameters for Advanced Ceramics." West Conshohocken, PA, ASTM International, 2013. (ASTM C1239-13.)

3. ASTM International. "Standard Test Method for Monotonic Equibiaxial Flexural Strength of Advanced Ceramics at Ambient Temperature." West Conshohocken, PA, ASTM International, 2013. (ASTM C1499-09.)

4. J. A. Salem and M. Adams. "The Multiaxial Strength of Tungsten Carbide," *Ceramic Eng. Sci. Proc.*, Vol. 20, (1999), pp. 459–466.

5. M. Ambrožič and L. Gorjan. "Reliability of a Weibull Analysis Using Maximum-Likelihood Method," *J. Mater. Sci.*, Vol. 46, (2011), pp. 1862–1869.

6. D. R. Thoman, L. J. Bain, and C. E. Antle. "Inferences on the Parameters of the Weibull Distribution," *Technometrics,* Vol. 11, (1969), pp. 445–460.

7. ASTM International. "Standard Practice for Size Scaling of Tensile Strengths Using Weibull Statistics for Advanced Ceramics." West Conshohocken, PA, ASTM International, 2015. (ASTM C1683-10.)

8. C. A. Klein, R. P. Miller, and R. L. Gentilman. "Characteristic Strength and Weibull Modulus of Selected Infrared-Transmitting Materials," *Opt. Eng.*, Vol. 41, (2002), pp. 3151–3160.

9. C. T. Warner, T. M. Hartnett, D. Fisher, and W. Sunne. "Characterization of ALON^{TM} Optical Ceramic," *Proc. SPIE*, Vol. 5786, (2005), pp. 95–109.

10. C. A. Klein. "Flexural Strength of Infrared-Transmitting Window Materials: Bimodal Weibull Statistical Analysis," *Opt. Eng.*, Vol. 50, (2011), p. 023402.

11. G. A. Graves, J. Wimmer, and D. McCullum. "Exploratory Development on Multidisciplinary Characterization of Infrared Transmitting Materials." Dayton, OH, University of Dayton Research Institute, 1979. (Rept. No. AFML-TR-4152.)

12. C. A. Klein. "Calcium Fluoride Windows for High-Energy Chemical Lasers," *J. Appl. Phys.*, Vol. 100, (2006), p. 083101.

13. J. Larkin, N. Klausutis, R, Hilton, and J. Adamski. *Proc. 5th Conf. Infrared Laser Window Materials, December 1975*. Arlington, VA, Defense Advanced Research Projects Agency, 1976, pp. 1079–1085.

14. A. R. Davies, J. E. Field, and C. S. J. Pickles. "Strength of Free-Standing Chemically Vapour-Deposited Diamond Measured by a Range of Techniques," *Phil. Mag.*, Vol. 83, (2003), pp. 4059–4070.

15. J. A. Detrio, D. J. Iden, F. Orazio, S. Goodrich, and G. Shaughnessy. "Experimental Validation of the Weibull Area Scaling Principle," *Proc. 12th DoD Electromagnetic Window Symposium*, Redstone Arsenal, AL, 2008.

16. W. F. Adler and D. J. Mihora. "Biaxial Flexure Testing: Analysis and Experimental Results," in *Fracture Mechanics of Ceramics,* Vol. 10, ed. by R. C. Bradt, D. P. H. Hasselman, D. Munz, M. Sakai, and V. Y. Shevchenko. Plenum Publishing Corp., New York, 1992.

17. J. Salem, R. Rogers, and E. Baker. "Structural Design Parameters for Germanium," *Proc. 15th DoD Electromagnetic Windows Symposium*, Arlington, VA, 2016.

18. Naval Weapons Center. *Evaluation of Statistical Fracture Criteria for Magnesium Fluoride Seeker Domes*, by M. D. Herr and W. R. Compton. China Lake, CA, NWC, 1980. (NWC TP 6226, publication UNCLASSIFIED.)

19. R. W. Sparrow, H. Herzig, W. V. Medenica, and M. J. Viens. "Influence of Processing Techniques on the VUV Transmittance and Mechanical Properties of Magnesium Fluoride Crystal," *Proc. SPIE*, Vol. 2286, (1994), pp. 33–45.

20. D. C. Harris, L. R. Cambrea, L. F. Johnson, R. Seaver, M. Baronowski, R. Gentilman, C. S. Nordahl, T. Gattuso, S. Silberstein, P. Rogan, T. Hartnett, B. Zelinski, W. Sunne, E. Fest, W. H. Poisl, C. B. Willingham, G. Turri, M. Bass, D. Zelmon, and S. M. Goodrich. "Properties of an Infrared-Transparent MgO-Y_2O_3 Nanocomposite," *J. Am. Ceram. Soc.*, Vol. 96, (2013), pp. 3828–3835.

21. M. Parish, M. Pascucci, N. Corbin, B. Puputti, G. Chery, and J. Small. "Transparent Ceramics for Demanding Optical Applications," *Proc. SPIE,* Vol. 8016, (2011), p. 80160B.

22. M. V. Parish, M. R. Pascucci, and W. H. Rhodes. "Aerodynamic IR Domes of Polycrystalline Alumina," *Proc. SPIE,* Vol. 5786, (2005), pp. 195–205.

23. M. V. Parish and M. R. Pascucci. "Polycrystalline Alumina for Aerodynamic IR Domes and Windows," *Proc. SPIE*, Vol. 7302, (2009), p. 730205.

24. M. R. Borden and J. Askinazi. "Improving Sapphire Window Strength," *Proc. SPIE,* Vol. 3060, (1997), pp. 246–249.

25. L. M. Belyayev, ed. *Ruby and Sapphire*. Nauk Publishers, Moscow, 1974, p. 321. English translation by P. M. Rao, Amerind Publishing Co, New Delhi. Available from U.S. National Technical Information Service, Springfield, VA.

26. T. M. Regan, D. C. Harris, D. W. Blodgett, K. C. Baldwin, J. A. Miragliotta, M. E. Thomas, M. J. Linevsky, J. W. Giles, T. A. Kennedy, M. Fatemi, D. R. Black, and K. P. D. Lagerlöf. "Neutron Irradiation for Sapphire Compressive Strengthening: II. Physical Property Changes," *J. Nucl. Mater.*, Vol. 300, (2002), pp. 46–56.

27. J. W. Fischer, W. R. Compton, N. Jaeger, and D. C. Harris. "Strength of Sapphire as a Function of Temperature and Crystal Orientation," *Proc. SPIE*, Vol. 1326, (1990), p. 11.

28. F. Schmid and D. C. Harris. "Effects of Crystal Orientation and Temperature on the Strength of Sapphire," *J. Am. Ceram. Soc.*, Vol. 81, (1998), p. 885.

29. S. M. Sweeney, M. K. Brun, T. J. Yosenick, A. Kebbede, and M. Manoharan. "High Strength Transparent Spinel With Fine, Unimodal Grain Size," *Proc. SPIE,* Vol. 7302, (2009), p. 73020G.

30. W. J. Tropf and D. C. Harris. "Mechanical, Thermal, and Optical Properties of Yttria and Lanthana-Doped Yttria," *Proc. SPIE,* Vol. 1112, (1989), pp. 9–19.

31. R. L. Gentilman. "New and Emerging Materials for 3–5 Micron IR Transmission," *Proc. SPIE,* Vol. 683, (1986), pp. 2–11.

32. W. H. Rhodes, G. C. Wei, and E. A. Trickett. "Lanthana-Doped Yttria: A New Infrared Material," *Proc. SPIE,* Vol. 683, (1986), pp. 12–18.

33. J. A. Salem, "Mechanical characterization of ZnSe windows for use with the FENIACS module," NASA/TM—2006-214100.

34. Southern Research Institute Report. *Biaxial Flexural Evaluations of Zinc Sulfide*. Birmingham, AL, SRI, October 1988. (SRI-MME-88-259-6270, publication UNCLASSIFIED.)

35. D. C. Harris, M. Baronowski, L. K. Henneman, L. LaCroix, C. Wilson, S. Kurzius, B. Burns, K. Kitagawa, J. Gembarovic, S. M. Goodrich, C. Staats, and J. J. Mecholsky, Jr. "Thermal, Structural, and Optical Properties of Multispectral Zinc Sulfide (Cleartran®)," *Opt. Eng.*, Vol. 47, (2008), p. 114001.

36. A. Krell, P. Blank, H. Ma, T. Hutzler, M. P. B. van Bruggen, and R. Apetz. "Transparent Sintered Corundum With High Hardness and Strength," *J. Am. Ceram. Soc.*, Vol. 86, (2003), pp. 12–18.

37. A. Krell, P. Blank, H. Ma, T. Hutzler, and M. Nebelung. "Processing of High-Density Submicrometer Al_2O_3 for New Applications," *J. Am. Ceram. Soc.*, Vol. 86, (2003), pp. 546–553.

38. A. Krell, G. Baur, and C. Dähne. "Transparent Sintered Sub-µm Al_2O_3 With IR Transmissivity Equal to Sapphire," *Proc. SPIE,* Vol. 5078, (2003), pp. 199–207.

39. R. Apetz and M. P. B. van Bruggen. "Transparent Alumina: A Light Scattering Model," *J. Am. Ceram. Soc.*, Vol. 86, (2003), pp. 480–486.

40. G. Bernard-Granger, C. Guizard, and N. Monchalin. "Sintering of an Ultrapure α-Alumina Powder: II. Mechanical, Thermo-Mechanical, Optical Properties and Missile Dome Design," *Int. J. Appl. Ceram. Technol*., Vol. 8, (2009), pp. 366–382.

This page intentionally left blank.

INITIAL DISTRIBUTION

1   Defense Technical Information Center, Fort Belvoir, VA

ON-SITE DISTRIBUTION

4   Code 4G0000D (archive and file copies)
7   Code 4F0000D, Harris, D.